Biomech Model Mechanobiol (2010) 9:573–581
DOI 10.1007/s10237-010-0198-6

ORIGINAL PAPER

A computational biomimetic study of cell crawling

Sitikantha Roy · H. Jerry Qi

Received: 27 July 2009 / Accepted: 25 January 2010 / Published online: 4 March 2010

Abstract Cell locomotion is a result of a series of synchronized chemo-mechanical processes. Previous extensive experimental studies have revealed many chemo-mechanical processes that may contribute to cell locomotion. In parallel, theoretical works have been developed to provide deeper insight. To date, however, direct simulations of cell locomotion on a substrate have not been seen. In this paper, a finite element–based computational model is developed to study amoeboid type of cell crawling phenomenon. Here, a cell is modeled as a 2D fluid-filled elastic vesicle, which establishes its interaction with a rigid substrate through a kinetics-based cellular adhesion model. The cell derives its motion through a differential bond breaking at the trailing edge and bond formation at the leading edge. This mechanism of crawling authenticates the hypothesis that cell locomotion can be facilitated by breaking the adhesive bonds at the rear edge, which was initially proposed by Chen (J Cell Biol 90: 187–200, 1981).

Keywords Cell crawling · Cell motility · Computational modeling of cells · Finite element modeling of cells

1 Introduction

The importance of the study of cell migration originates from its necessity in various biological processes to maintain proper homeostasis (Ananthakrishnan and Ehrlicher 2007; Lodish and Darnell 1995). For example, in a multicellular organism, during morphogenesis, dividing cells move to specific sites to form tissues and organs (Stossel 1993). During wound healing, fibroblasts crawl toward the wound to reconstruct damaged tissues (Bray 2001). Human immune system is a highly coordinated activity dependent on white blood cell's crawling on the endothelial layer, which forms the inner lining of the blood vessel (Lodish and Darnell 1995). Uncontrolled cell migration through tissues occurs during cancer metastasis (Alberts 2008). Defective cell migration also lead to pathological consequences like auto-immune diseases (Lodish and Darnell 1995). Over the last few decades, experimental research on cell migration has improved our understanding about the various complex biomechanical and biochemical activities involved in cell locomotion (Lauffenburger and Horwitz 1996). However, due to the complicated nature of cell locomotion and difficulty in expressing biological observations into mathematical descriptions (Mogilner 2009), we still lack quantitative understanding through predictive theoretical models (Flaherty et al. 2007). Quantification is particularly necessary to gain insight on how a cell derives its motion at the micrometer scale through the molecular level chemo-mechanical changes. Review papers such as Flaherty et al. (2007) discuss the existing modeling ideas at the continuum scale, while Mogilner (2009) gives a summary of the existing models of cell crawling from a bottom-up perspective and discusses how the molecular details add up to create motion at the continuum scale.

Cell migration can take different forms, such as "swimming," inch-worming, and gliding (Bray 2001). Crawling is a specialized type of movement mechanism and is commonly seen in cells which reside on surfaces or surface like physiological environment (Bray 2001). For example, extracellular matrix (ECM) provides a migrating platform for fibroblast kind of cell. Another example of unicellular species which adopts crawling mechanism to move is amoeba. The basic steps in amoeboid movement are the same for other types of

S. Roy · H. J. Qi (✉)
Department of Mechanical Engineering,
University of Colorado, Boulder, CO 80309, USA
e-mail: qih@colorado.edu

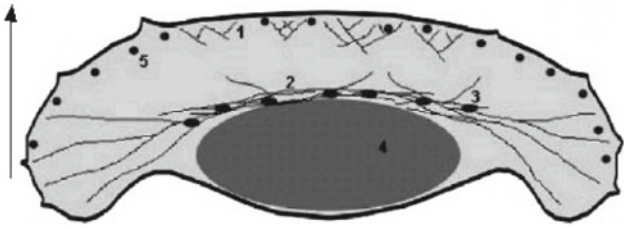

Fig. 1 The morphology of a migrating fish keratocyte (Rubinstein et al. 2005)

crawling cells and therefore amoeba is sometime taken as a model cell to understand crawling mechanism (Bray 2001; Gracheva and Othmer 2004).

In physiological environments, cell crawling is a very complex and multi-physical phenomenon, requiring coordinated activity of cytoskeleton, membrane, and adhesion system. One characteristic feature of amoeboid type of crawling mechanism is polarization, *i.e.* the development of a visible asymmetry between the leading edge and the trailing edge of a migrating cell (Lodish and Darnell 1995). From a macroscopic perspective, cell crawling process can be divided into three phases: protrusion, translocation, and retraction. During the protrusion phase, a migrating cell starts to be polarized and extends its membrane in the forward direction to form new adhesion sites. This membrane extension is commonly called lamellipodium, and at this time, a migrating cell takes a hand fan-like morphology (Fig. 1) with long axis perpendicular to the direction of migration (Munevar et al. 2001; Rubinstein et al. 2005). In the translocation phase, the contractile machinery inside the cell activates and pulls up the rearward portion of the cell body forward. In the retraction phase, cell de-bonds the mature focal contacts in its rear end to move forward. However, the exact mechanism by which these three phases are related and added up to produce forward movement is not clear yet. One hypothesis is that formation of new contacts during the protrusion phase produces a tethering kind of contractile force in the cell body, and during the subsequent de-adhesion in the trailing edge, it elastically retracts towards the forward direction. This resembles stretching a rubber band and sticking it at the front and then releasing the rear end. In this hypothesis, protrusion is assumed to be the cause, and retraction is the effect and commonly referred as "frontal towing mechanism" in the literature (Munevar et al. 2001a). The contractile force at the rear is generated in part due to the elastic nature of the cell membrane and the rest due to the active force generated by the actin-myosin contractile machinery (cytoskeleton network) inside the cell. Another hypothesis, in which retraction is assumed to be the active process and accelerated protrusion, is observed to occur due to the detachment at the trailing edge, commonly termed as "retraction induced spreading" in the literature (Chen 1979). These two hypotheses focus on different aspects of cell crawling and appear to be a controversy. In an actual situation, it is probably a complex combination of mechanisms based on both of these hypotheses that drive a cell forward.

In this paper, we study the cell crawling phenomenon of an adherent cell on a rigid substrate by a finite element (FE)–based model. We model the cell as a 2D vesicle made of an elastic material which is a coarse-grained biomimetic representation of an actual cell. The substrate is modeled as a rigid base. We neglect the molecular details inside the cell, such as the elasticity originated from cytoskeleton remodeling and stress fiber formation, and myosin II activated cell contractile force (Lodish and Darnell 1995). The cell crawling process is studied through two sequential steps: In the first step, the cell spreads over the substrate from suspension and forms a stable focal adhesion zone. After the stable spreading, de-bonding at the trailing edge of the focal adhesion zone is introduced at a certain rate, which results in cell crawling on the substrate in a tank-thread manner.

2 Model description

In the present model, two distinct length scales exist: one is the adhesion bond-length-scale, which is of nanometer size, and the other is the cellular length-scale, which is of micrometer size. Our main objective in the present case is to bridge these two distinct length scales involved in cell migration process.

2.1 Adhesion model/nano-scale model

In order to start crawling on a substrate, a cell first needs to adhere to the surface. There are some well-known vesicle-substrate adhesion models existing in the literature (Hammer and Tirrell 1996; Zhu et al. 2000; Zhu 2000). To model the mechanics and kinetics of adhesion, we adopt a simple traction-separation relation (Liu et al. 2007) between the receptors in the cell membrane and the ligands on the substrate surface. The kinetics of the bond formation is adopted from Bell (1978). The traction-separation relation is assumed to follow a potential function given as Seifert (1991)

$$\Phi(h) = \gamma \left[\left(\frac{\varepsilon}{h}\right)^4 - 2\left(\frac{\varepsilon}{h}\right)^2 \right], \tag{1}$$

where h is the separation between the cell surface and the rigid base, and ε is the depth of the attractive well. The potential expression in Eq. (1) gives a lumped effect of the adhesion bond strength. We do not differentiate between the non-specific and specific bond forces (Bell 1978) in the present case. Also, we assume that the receptor density over the cell membrane, as well as the ligand density on the rigid substrate, is spatially uniform. The effect of diffusion on the receptor

mobility on the cell membrane and its subsequent effect on migration are not considered in the current model. They are currently studied by the authors and will be reported in the future. The receptor-ligand bond formation follows a kinetics law given as (Bell 1978),

$$\frac{\partial N_b}{\partial t} = k_f(N_{l0} - N_b)(N_{r0} - N_b) - k_r N_b, \tag{2}$$

where N_b is the bond density, k_r and k_f are the reverse and forward reaction rate coefficients, respectively. N_{l0} is the initial ligand density on the rigid base, and N_{r0} is the initial density of receptor on the cell membrane (N'dri et al. 2003). The normal adhesive/repulsive stress between the membrane and the surface is calculated as

$$f_n = -N_b \nabla_h(\Phi). \tag{3}$$

We also include a horizontal component of the force to resist the slippage of the vesicle membrane on the substrate. This horizontal force is defined as $f_h = -\bar{c}_k \delta_h$, where δ_h is the accumulated total horizontal displacement of the nodes in the contact zone on the cell surface and $\bar{c}_k$ is a constant. A more realistic traction-separation relation, like the one developed by Reboux et al. (2008), where the orientation of the receptor-ligand bonds is taken into account, can be implemented into the present model. In the present case, we define the contact zone as the region of the cell which lies within the 20 nm distance from the surface. The horizontal force f_h is assumed to arise from the focal adhesion complexes in the actual physiological condition (Reboux et al. 2008). This interaction model was implemented as a user subroutine VUINTER in a finite element software package ABAQUS (2007) Explicit (SIMULIA, Providence, RI).

2.2 Macro-scale cellular model

The cell is modeled as a fluid-filled 2D elastic ring with a diameter of 8μm (Reboux et al. 2008). The present model is a 2D idealization of an actual cell, where the membrane is modeled as beam elements (B21, a two-node linear element in ABAQUS (2007) finite element setup). We modeled the cell membrane as made of elastic material with two independent material constants: a typical Young's modulus value of 9,000 Pa (Bao and Suresh 2003) and Poisson's ratio of 0.4. The beam elements were assumed to have a unit out-of-plane thickness, and the height of the beam was chosen to be 20 nm. The combination of Young's modulus and the beam height yields a bending stiffness of $\sim 1.7 \times 10^{-20}$ Nm, which is in the range of bending stiffness for cell membrane (Mohandas and Evans 1994). The transverse shear effect is assumed to be negligible (Cheng et al. 2009). When the cell deforms, the elastic energy of deformation is stored both in bending and axial modes. In order to model the pressure exerted by the enclosed fluid during the deformation of the cell membrane, we follow a similar approach as in Liu et al. (2007) and model the fluid inside the vesicle cavity as incompressible by choosing a very high bulk modulus of fluid, and assume it to be homogeneous in composition and density. The enclosed area filled up by the cytoplasm remains constant during the deformation but the pressure may change. The temperature and the fluid pressure are assumed to be uniform (Liu et al. 2007). The viscosity of the fluid is neglected (Evans and Hochmuth 1976). ABAQUS (2007) Explicit solves the coupled fluid structure interaction problem through its fluid cavity modeling capability. It is important to mention that a better approximation of cell would be elastic membrane filled with Stokesian fluid. The main reason to choose Eulerian (non-viscous) fluid in our simulations is because the limitation of ABAQUS (2007), which currently only offers a very limited fluid-solid coupling capability. However, we also note that in studies by Evans and Hochmuth (1976), it has been found that the viscous energy dissipation of the cytoplasm is very small; in that regard using Eulerian fluid may also provide a good approximation of cytosol. Because of this, Eulerian fluid was used in several recent studies on cell mechanics and cell–substrate interaction (Liu et al. 2007; Cheng et al. 2009; Zhang and Zhang 2008; Dao et al. 2003; Lim et al. 2004). The initial configuration is chosen as a 2D circular vesicle making a point contact with the substrate. In the first step (STEP I), the cell spreads over the surface by forming focal adhesion zone through receptor-ligand bonds following the traction-separation rule defined by Eqs. 1–3. The kinetic energy of the system is damped out to zero at the end of the STEP I so that a stable focal adhesion zone is established. As the present simulation is a quasi static analysis, we use a mass scaling scheme (ABAQUS 2007) to expedite the simulation speed. In the second step (STEP II), receptor-ligand bond at the rear end of the vesicle starts to break. Here, we assume that the interaction between the substrate and the rear end (the left most node, Fig. 2) in the focal adhesion zone diminishes in t_b seconds. For implementing it numerically, we reduce the bond density (N_b) of the left most node in a linear manner over t_b seconds

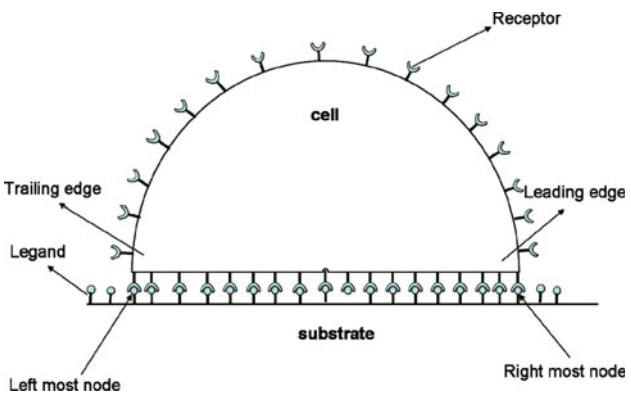

Fig. 2 Schematic of vesicle adhesion through receptor-ligand bond formation

Table 1 The system parameters and their literature values

Symbol	Definition	Typical model value	Range	References
$R\,\mu$m	Cell radius	4.0	4.0–8.0	Reboux et al. (2008)
λ (nm)	Bond length	20	10–300	Springer et al. (1990)
N_{r0} ($1/\mu m^2$)	Free receptor density	10,000	10^2–10^4	Liu et al. (2007)
N_{l0} ($1/\mu m^2$)	Free ligand density	10,000	10^3–10^4	Liu et al. (2007)
E (Pa or pN/μm^2)	Membrane young's modulus	9,000	10^2–10^5	Bao and Suresh (2003)
δ_c (μm)	Cutoff distance	0.02	0.06–0.8	Liu et al. (2007)
k_f ($s^{-1}\mu m^2$)	Forward reaction rate	1.0×10^{-4}	10^2–1.0×10^{-4}	Zhang et al. (2008)
k_r (s^{-1})	Reverse reaction rate	1.0×10^{-6}	1.0×10^{-2}–10^{-6}	
D (nm)	Membrane thickness	20	10–20	Zhang et al. (2008)
γ (pN $-$ μm)	Parameter in Eq. 1	0.024	0.024	
ε (μm)	Parameter in Eq. 1	0.01	0.01	
$\bar{c}_k$ (pN/μm^2)	Horizontal shear parameter	60	60	

and thus from Eq. 3, the normal stress drops down to zero over this time interval. Immediately after that interaction breaks, the interaction at the new rear end (the new left most node) starts to diminish. This bond-breaking process repeats and is automated through the computer code. Here, we assume that breaking bonds or de-adhesion at the rear end is caused by certain chemo-mechanical coupling, such as myosin- generated contractile force (Lodish and Darnell 1995) and its effect on the de-adhesion rate. Models considering the molecular details of bond breaking are a further step of development. In the present case, we assume that varying the magnitude of the force, cell can vary the de-adhesion rate at the rear end.

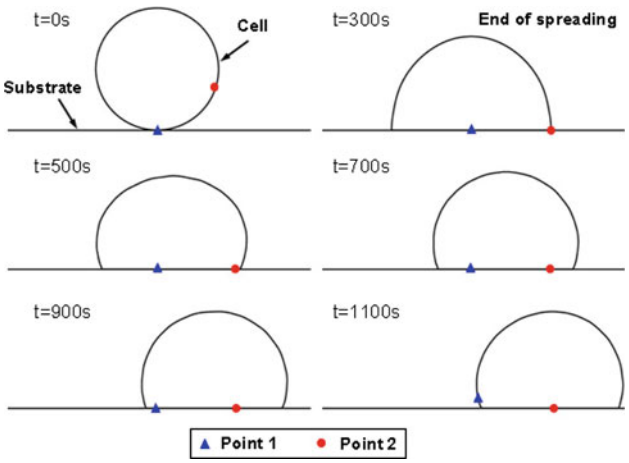

Fig. 3 Snapshots of cell crawling due to de-adhesion at the rear end. The end of STEP I is at $t = 150$ s

3 Results

The finite-element software ABAQUS (2007) was used as the platform for the model development. The traction-separation rule described by Eqs. 1–3 was implemented into a user interface subroutine VUINTER. The user subroutine also automated the de-adhesion rate at the rear end in the second step of the simulation. For the presentation of the simulation results, we used a similar normalizing scheme as adopted by Liu et al. (2007), where length was normalized by the diameter of the vesicle, a_0; energy by $E_0 = k_B T_R$, where k_B is the Boltzmann constant and T_R is the room temperature; force by $F_0 = E_0/a_0$; and stress by $\sigma_0 = F_0/a_0^2$.

3.1 A typical case study

For a typical case study, we take the values of the parameter listed in Table 1, under the column heading entitled "Typical model value." The bond-breaking parameter t_b is assumed to be the same, 4.5 s.

Figure 3 shows the snapshots of cell shape and position in the simulation. The end of STEP I is at $t = 300$ s. It is remarkable that just by breaking bonds at the rear end in STEP II, the entire cell body can move forward. In these snapshots, the positions of two nodes are highlighted by an arrow symbol and a round symbol, respectively. It can be seen that the positions of these nodes do not move until their adhesions to the substrate break. This indicates that the vesicle moves in a tank-thread manner. Figure 4a shows the variation of the coordinates of the right most node and the left most node in the contact zone during migration phase, and Fig. 4b shows the contact length evolution of the vesicle with time. Oscillations in contact length are observed. This may be partly due to the instability of the central difference algorithm adopted in ABAQUS (2007) Explicit and the rest due to the dynamic nature of the problem. The whole migration process can be grouped into three successive stages: spreading, transition, and stabilization. During the spreading phase, the

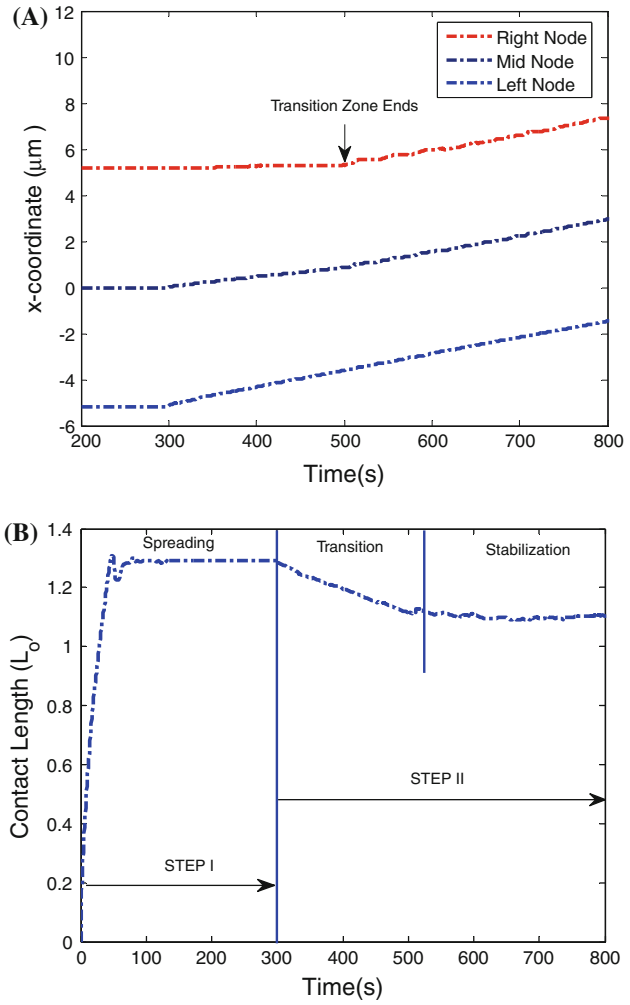

Fig. 4 **a** The variation of x-coordinate of the *left* most node and the *right* most node at the contact region with time, for $t_b = 4.5$ s. **b** Contact length evolution with time

vesicle spreads over the surface from suspension and becomes stabilized after a certain time (Fig. 3, $t = 300$ s). In STEP II, the bonds in the rear end start to break; the formation of new bonds in the forward side does not start until the elastic energy released due to bond breaking at the rear end reaches a certain level. The formation of new bond leads to the growth of adhesion front and the forward motion of the cell. This is similar to the experimentally observed fact that retraction of a migrating fibroblast tail leads to accelerated protrusion at the cell front (Chen 1981a). At the initial stage of the second step, new bond does not form. This leads to a reduction in cell contact length (or spreading area) (Fig. 4) and a slight change in cell shape (Fig. 3, $t = 500$ s and $t = 700$ s correspond to the middle and the end of transition, respectively). It also can be seen that cell shape becomes slightly asymmetric as the cell starts to shift its center of mass. The transition zone diminishes as the new bonds start to form and the cell starts to crawl in the forward direction with a uniform speed (Fig. 3, $t = 900$ s and $t = 1{,}100$ s). The stabilized zone indicates that the rate of retraction becomes equal to the rate of protrusion at the front and the cell reaches a dynamic equilibrium (Dunn and Zicha 1995). The contact length of the cell is determined by the balance between the rates of bond breaking at the trailing edge and elastic energy release rate, which dictates the rates of bond formation at the leading edge (Dunn and Zicha 1995). In actual physiological situation, the difference between the rate of bond breaking at the rear and the rate of lamellipodial extension (new adhesion bond formation) leads to the formation of "ruffles," "blebs" on the cell surface (Chen 1981b).

It is a well-observed fact that cell exerts horizontal traction force during locomotion to pull on the surface of the substrate through its focal adhesion sites (Harris et al. 1980). For example, traction images of migrating 3T3 cells (Munevar et al. 2001b) indicated that due to polarization, strong tethering stresses appear at the leading edge during locomotion. In particular, those contacts that are immediately behind the front of the lamellipodium exert more force per unit area than those at the rear of the cell (Small et al. 2002). The horizontal traction force serves two purposes during amoeboid type of crawling locomotion; first it anchors the cell to the substrate and second it helps to drag the intracellular part in the forward direction, which is called translocation. Figure 5 shows the profile of the horizontal traction in the contact region during cell locomotion. The positive horizontal stress is defined along the positive x-direction as shown in Fig. 2. As shown in Fig. 5, the present model indicates an increasing trend in the stress magnitude in the vicinity of the leading edge when compared to the stress magnitude in the rear end. In addition, stress shows much higher variations in the vicinity of the leading edge, indicating a drastic vibration due to high stress in this region. In an actual migrating cell, a centripetal distribution of the stress profile (Tan et al. 2003) has been observed, and magnitude wise, it assumes a bowl kind of shape. The reason for this discrepancy might be due to the fact that we have only considered rearward de-adhesion, but in an actual physiological condition, other effects like pushing effect due to polymerization of the actin cortical layer in the front (ratchet mechanism) also contribute to the migration.

3.2 Effect of membrane stiffness

Figure 6 shows the evolution of the length of focal adhesion zone with varying membrane stiffness. It is observed that with increasing stiffness, the length of focal adhesion zone between the vesicle and the substrate decreases. This is because as the membrane is stiffer, more elastic energy is needed to deform the vesicle in order to establish the same length of focal adhesion zone. In the present case, the deformation energy is derived from the energy released during the

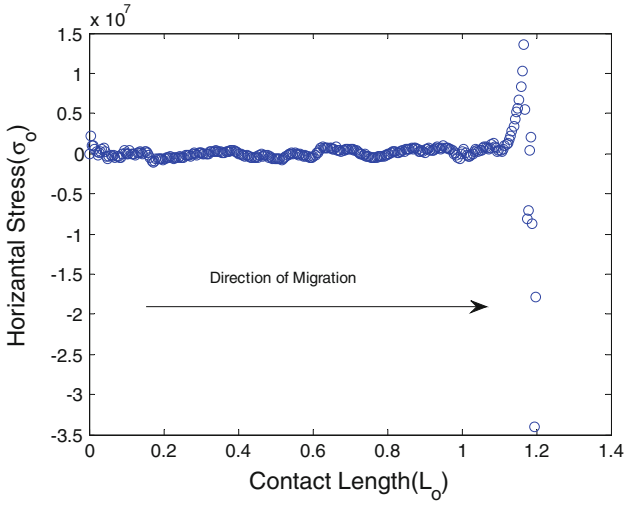

Fig. 5 The horizontal stress in the contact region at $t = 500$ s

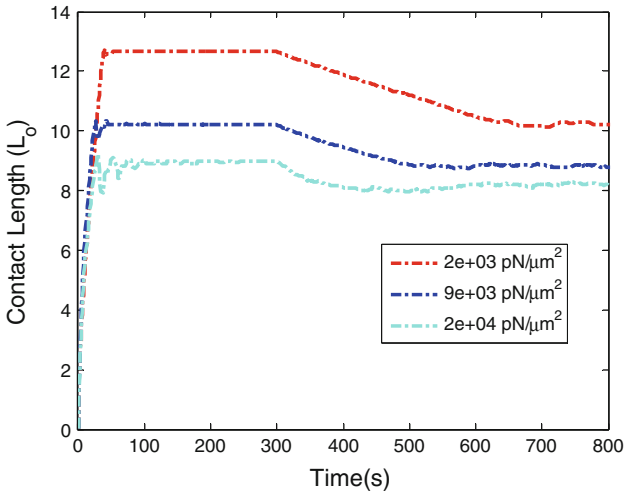

Fig. 6 The contact length evolution for varying membrane Young's modulus

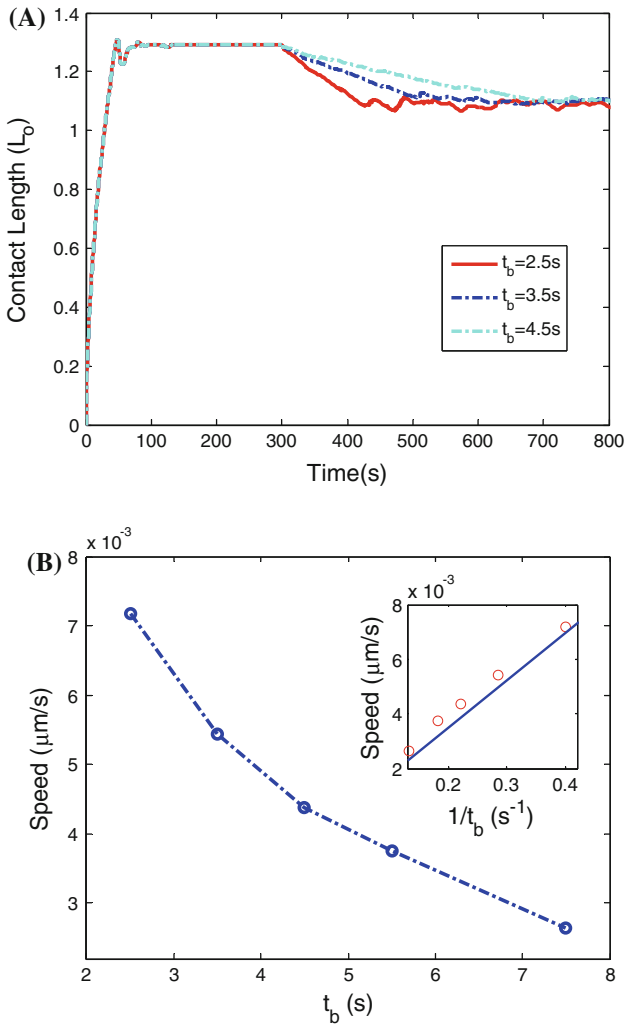

Fig. 7 **a** The contact length evolution with varying rate of bond breaking. **b** Steady state speed with different bond breaking rate

formation of adhesion bonds between the vesicle membrane and the substrate. The strength of the adhesion bonds is characterized by the value of γ in Eq. 1. As the adhesion strength remains constant, so with increasing membrane stiffness, the deformation of the vesicle reduces. Figure 6 also shows that the membrane stiffness has some effect on the "length of the transition period" before the vesicle attain its steady state speed. As the stiffness increases, the length of the transition zone decreases. This indicates that transition period is not only determined by the balance between bond-breaking rates at the rear end and the new bond formation rate at the leading end, but it also is a function of the membrane stiffness.

3.3 Effect of bond-breaking rates at the rear end

To study the effect of the rate of bond breaking at the rear end, we vary $t_b = 2.5$, 4.5, and 7.5 s. All other values are taken as those listed in Table 1. Figure 7a shows with increasing rate of de-adhesion at the rear, the length of the transition zone increases. Faster the rate of bond breaking, quicker it is for the cell to attain steady state speed. Fig. 7b shows the variation of the steady state speed with the rate of retraction at the rear end of the vesicle. It is intuitive that as the rate of retraction increases, the vesicle moves much faster during the steady state. Since at the stead state, the rate of de-bonding at the rear end should be equal to the rate of forming new bond at the leading edge in order to maintain a constant length of focal adhesion zone, the steady state velocity should be linearly proportional to $1/t_b$, as shown in the inset of Fig. 7b.

3.4 Effect of compressibility of the cytoplasm fluid

In the above studies, we have considered the cytoplasmic fluid inside the cell to be incompressible in nature. It is a

common practice in the current literatures (Liu et al. 2007; Cheng et al. 2009) to assume the cytoplasmic fluid inside the cell to be volume preserving (area preserving in 2D) or incompressible. When this incompressibility condition is imposed in the computation for a cell with an initial circular undeformed shape, the cell membrane cannot preserve its area (or length in 2D) during deformation. This is because a sphere (or circle in 2D) is a specific geometric shape which encloses the maximum volume (or area) under a minimum surface area (or peripheral length). A similar procedure was adopted (Liu et al. 2007; Cheng et al. 2009) to model a cell as a spherical vesicle in 3D, but in their work, the feasibility of simultaneous volume and surface area preservation was not explored. In our current simulation due to incompressible nature of the cytoplasm, the maximum axial stretch in the beam is about ∼15%. Such a stretch ratio is certainly unphysical, as a lipid bilayer will break before it reaches this stretch. To address this, we conducted another simulation where we assume the fluid is "compressible," so that the peripheral length of the cell membrane can be preserved. The compressibility of the fluid is quantified by its bulk modulus (with all other parameters remaining same as the typical case). It is observed that even with compressible fluid inside, the circular vesicle can move in a similar manner (Fig. 8a) as before, and the speed of locomotion is independent of its compressibility as the bulk modulus decreases until ∼10 pN/μm^2. When the bulk modulus is smaller than 10 pN/μm^2, the speed of cell locomotion increases. At the bulk modulus of 2 pN/μm^2, the speed is ∼40% more than the speed when the bulk modulus is above 10 pN/μm^2 (Fig. 8b). We also notice that when the bulk modulus is 2 pN/μm^2, the average axial stretch in the membrane is less than 3%, which is close to the case where the area of the cell membrane is conserved. In both cases, de-adhesion at the rear causes an asymmetric cell spreading (which is the basic physics behind retraction-induced protrusion hypothesis) and induces a polarized elastic energy distribution, which drives the vesicle forward. We therefore believe that this physics should not change, should we adopt more advanced membrane mechanics model and cell model. However, our model also shows that internal pressure due to cytosol does play a role in determining cell locomotion speed. Therefore, future studies should be conducted to investigate the influence of detailed cell properties, such as viscous effect of cytosol to the cell locomotion.

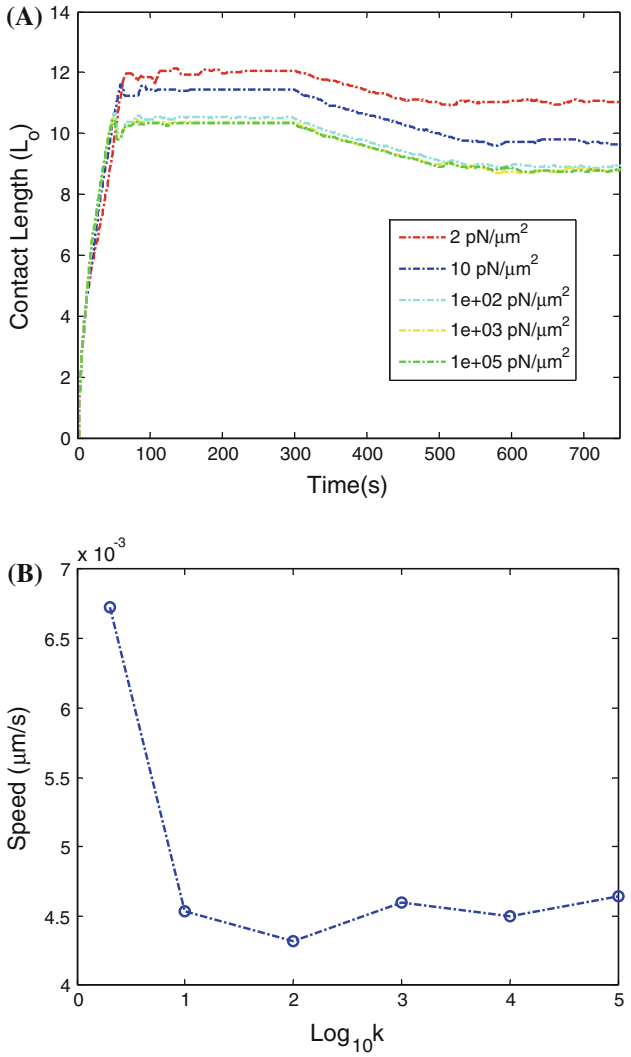

Fig. 8 **a** The contact length evolution with varying fluid bulk modulus inside the fluid cavity. **b** The speed of the cell with varying bulk modulus (k) of the fluid inside the fluid cavity

4 Discussions

Complexity of a biological phenomenon arises due to the presence of various coordinated processes at different length scales in a single activity, like cell crawling. Each of these processes also involves complex molecular level changes. Integrating all of these multi-scale processes into a unified model system is a challenge. A model which can capture all these macroscopic as well as molecular details is very complex, if not impossible. For simplified understanding, over the years biomimetic approaches, like the present one, have been very useful to study and derive insights about various cellular processes at the continuum scale (Smith and Sackmann 2009; Dong and Lei 2000). In addition, biomimetic study can help to establish a platform connecting biological principle with synthetic material development. For example, if we can understand and implement cellular crawling mechanism into a vesicular movement, we can implement it to synthetically develop self-healing material (Smith and Sackmann 2009).

The present model supports the hypothesis that among various possible propulsive mechanisms and their varied combinations, one of the mechanisms to derive forward motion is to break the bonds at the trailing edge. This mechanism,

commonly termed as "retraction- induced spreading" was first experimentally proven by Chen (1979). Chen carried out an in vitro experiment on embryonic chick heart fibroblast to study both naturally and artificially induced retraction of the trailing edge on cell spreading through a time-lapse cinemicrography technique. In both cases, he observed retraction in the trailing edge always induces maximum spreading in the diametrically opposite leading end. The observation was also important in understanding the mechanism behind cell's directional movement. It was hypothesized that cell preferentially rapture the adhesive bonds at the tail, followed by the conversion of the stored potential energy in a stretched cell body into kinetic energy for forward migration in a particular direction (Munevar et al. 2001b). Not many works exist in the literature that can give some explanations about how the fast-moving keratocytes and slow-moving fibroblast control their speed. Our model, by simply breaking the adhesive bonds at the trailing edge without considering molecular details, supports the hypothesis that rapturing the bonds at the tail can facilitate the directional motion. Our model also indicates that controlling the rate of bond breaking at the rear end is a viable mechanism in this regard. However, we also acknowledge that the current model does not rule out the possibility of cell locomotion driven by other mechanisms, such as the formation of new adhesions at the front by actin polymerization in the cortical zone which pushes the front towards the direction of motion (ratchet mechanism). In addition, cell locomotion is a complicated process where different chemo-mechanical processes play in a highly coordinated manner to generate locomotion. The present model is an initial attempt towards incorporating those complicated effects and will be explored in future. For example, instead of prescribing a de-bonding time t_b, one can incorporate certain chemical potentials to determine the rate of bonding breaking. This will help to gain additional insight into the underling physics of cell locomotion.

Mathematical modeling of cell crawling is still at its initial phase of development. Majority of the models existing in the literature are hypothesis driven and try to give reasoning to a particular phenomenon (at molecular scale or macro-scale) observed in cell crawling process. We are aware of the fact that a biomimetic study cannot represent an actual cell with all its physiological complexities, but still simplified models like the present one can shed light on a particular physics and increase our understanding in an incremental way to achieve an ultimate unification in the coming future. Future work should be conducted to improve the model by incorporating more sophisticated cell models. For example, the current model treats the cytoplasm as Eulerian fluid. However, using the cell crawling velocity of $7\times10^{-3}\,\mu$m/s, cell length of $10\,\mu$m, and kinematic viscosity of $1\times10^{6}\,\mu\text{m}^2$/s, the Reynolds number is calculated to be 7×10^{-8}, indicating the relative importance of the viscous force over the inertial force. Therefore, Eulerian fluid cannot provide a correct representation of cytoplasm. Although the fundamental physics will not change, better representation of cytoplasm, such as using Stokesian fluid, should be used to provide better quantitative insight. In addition, a circular (or spherical) cell might not be a good model for cell to start with. Although this kind of shape does offer the advantage of simplicity for model development and has been adopted by other researchers (Liu et al. 2007; Cheng et al. 2009), for more advanced model, a non-spherical initial shape might be used so that the cell can maintain both the incompressible nature of the cytoplasm as well as the instretchability of its lipid membrane. With improved model, a systematic study can be conducted to evaluate the influence of the cytosol properties on the cell locomotion and how energy dissipation mechanism can affect cell locomotion.

Models in the initial phase of development of a scientific process, like cell crawling, become useful if they are developed in a modular basis (Flaherty et al. 2007) and leave plenty of opportunity for future update as our understanding grows. The present model does not deal with the origin of the contractile force to break the left most node and the mechanism by which cell controls it. As a future update, a contractile mechanism connecting the bond breaking with biochemical changes inside can be incorporated like Huxley's sliding filament model of mussel contraction (Lodish and Darnell 1995). Also, new ideas like viewing the cytoplasm as gel kind of material with a self-generated swelling pressure gradient between the leading edge and the trailing edge (Joanny et al. 2003; Mogilner and Oster 2003) can be combined to account for the physics of treadmilling observed in the cytoskeleton molecules and its effect in generation of the contractile force. It is also well established that cells do respond to changes in its mechanical environment, like the influence of substrate stiffness (Lazopoulos and Stamenovic 2008). The present modeling framework gives a platform to study these in future. Another update is to upgrade the model to a 3D vesicle, where we can study the directional movement of an adherent cell.

Acknowledgments The authors gratefully acknowledge for the financial support by NSF CMMI-0528548 and CMMI-0928067. The authors also acknowledge helpful suggestions from the reviewers.

References

ABAQUS (2007) User's manual, version 6.7, ABAQUS Inc., Pawtucket

Alberts B (2008) Molecular biology of the cell, 5th edn. Garland Science, New York. 1 v (various pagings)

Ananthakrishnan R, Ehrlicher A (2007) The forces behind cell movement. Int J Biol Sci 3(5):303–317

Bao G, Suresh S (2003) Cell and molecular mechanics of biological materials. Nat Mater 2(11):715–725

Bell GI (1978) Models for specific adhesion of cells to cells. Science 200(4342):618–627
Bray D (2001) Cell movements: from molecules to motility, 2nd edn. Garland Pub., New York, xiv, p 372
Chen WT (1979) Induction of spreading during fibroblast movement. J Cell Biol 81:684–691
Chen WT (1981a) Mechanism of retraction of the trailing edge during fibroblast movement. J Cell Biol 90:187–200
Chen WT (1981b) Surface changes during retraction induced spreading of fibroblast. J Cell Sci 49:1–13
Cheng QH et al (2009) A computational modeling for micropipette-manipulated cell detachment from a substrate mediated by receptor-ligand binding. J Mech Phys Solids 57(2):205–220
Dao M, Lim CT, Suresh S (2003) Mechanics of the human red blood cell deformed by optical tweezers. J Mech Phys Solids 51(11-12):2259–2280
Dong C, Lei XX (2000) Biomechanics of cell rolling: shear flow, cell-surface adhesion, and cell deformability. J Biomech 33(1):35–43
Dunn GA, Zicha D (1995) Dynamics of fibroblast spreading. J Cell Sci 108:1239–1249
Evans EA, Hochmuth RM (1976) Membrane viscoelasticity. Biophys J 16(1):1–11
Flaherty B, McGarry JP, McHugh PE (2007) Mathematical models of cell motility. Cell Biochem Biophys 49(1):14–28
Gracheva ME, Othmer HG (2004) A continuum model of motility in ameboid cells. Bull Math Biol 66(1):167–193
Hammer DA, Tirrell M (1996) Biological adhesion at interfaces. Ann Rev Mater Sci 26:651–691
Harris AK, Wild P, Stopak D (1980) Silicone-rubber substrata—new wrinkle in the study of cell locomotion. Science 208(4440): 177–179
Joanny JF, Julicher F, Prost J (2003) Motion of an adhesive gel in a swelling gradient: a mechanism for cell locomotion. Phys Rev Lett 90(16):168102
Kessler MR, Sottos NR, White SR (2003) Self-healing structural composite materials. Compos Part A-Appl Sci Manuf 34(8):743–753
Lauffenburger DA, Horwitz AF (1996) Cell migration: a physically integrated molecular process. Cell 84(3):359–369
Lazopoulos KA, Stamenovic D (2008) Durotaxis as an elastic stability phenomenon. J Biomech 41(6):1289–1294
Lim CT et al (2004) Large deformation of living cells using laser traps (vol. 52, p. 1837, 2004). Acta Mater 52(13):4065–4066
Liu P et al (2007) Simulations of the spreading of a vesicle on a substrate surface mediated by receptor-ligand binding. J Mech Phys Solids 55(6):1166–1181
Lodish HF, Darnell JE (1995) Molecular cell biology, 3rd edn. Scientific American Books: Distributed by W.H. Freeman and Co., New York. 1 v (various pagings)
Mohandas N, Evans E (1994) Mechanical-properties of the red-cell membrane in relation to molecular-structure and genetic-defects. Ann Rev Biophys Biomol Struc 23:787–818
Mogilner A (2009) Mathematics of cell motility: have we got its number? J Math Biol 58(1–2):105–134
Mogilner A, Oster G (2003) Shrinking gels pull cells. Science 302(5649):1340–1341
Munevar S, Wang YL, Dembo M (2001) Traction force microscopy of migrating normal and H-ras transformed 3T3 fibroblasts. Biophys J 80(4):1744–1757
Munevar S, Wang YL, Dembo M (2001a) Imaging traction forces generated by migrating fibroblasts. Biophys J 80(1):276A–276A
Munevar S, Wang YL, Dembo M (2001b) Distinct roles of frontal and rear cell-substrate adhesions in fibroblast migration. Mole Biol Cell 12(12):3947–3954
N'dri NA, Shyy W, Tran-Soy-Tay R (2003) Computational modeling of cell adhesion and movement using a continuum-kinetics approach. Biophys J 85(4):2273–2286
Reboux S, Richardson G, Jensen OE, (2008) Bond tilting and sliding friction in a model of cell adhesion. Proc Royal Soc A-Math Phys Eng Sci 464(2090):447–467
Rubinstein B, Jacobson K, Mogilner A (2005) Multiscale two-dimensional modeling of a motile simple-shaped cell. Multiscale Model Simul 3(2):413–439
Seifert U (1991) Adhesion of vesicles in 2 dimensions. Phys Rev A 43(12):6803–6814
Small JV et al (2002) How do microtubules guide migrating cells? Nat Rev Mole Cell Biol 3(12):957–964
Smith AS, Sackmann E (2009) Progress in mimetic studies of cell adhesion and the mechanosensing. Chemphyschem 10(1):66–78
Springer TA (1990) Adhesion receptors of the immune-system. Nature 346(6283):425–434
Stossel TP (1993) On the crawling of animal-cells. Science 260(5111): 1086–1094
Tan JL et al (2003) Cells lying on a bed of microneedles: an approach to isolate mechanical force. Proc Natl Acad Sci US Am 100(4):1484–1489
Zhang CY, Zhang YW (2008) Computational analysis of adhesion force in the indentation of cells using atomic force microscopy. Physical Review E 77(2)
Zhu C (2000) Kinetics and mechanics of cell adhesion. J Biomech 33(1):23–33
Zhu C, Bao G, Wang N (2000) Cell mechanics: mechanical response, cell adhesion, and molecular deformation. Ann Rev Biomed Eng 2:189–226